

EXPERIMENTAL AND REGRESSION ANALYSIS FOR MULTI CYLINDER DIESEL ENGINE OPERATED WITH HYBRID FUEL BLENDS

by

**Rajendiran GOPAL^{a*}, Mayilsamy KAVANDAPPA GOUNDAR^b,
Subramanian RAMASAMY^b, Nedunchezian NATARAJAN^b,
and Venkatachalam RAMASAMY^b**

^a Tamil Nadu College of Engineering, Coimbatore, Tamil Nadu, India

^b Institute of Road and Transport Technology, Erode, Tamil Nadu, India

Original scientific paper

DOI: 10.2298/TSCI130130127G

The purpose of this research work is to build a multiple linear regression model for the characteristics of multicylinder diesel engine using multicomponent blends (diesel-pungamia methyl ester-ethanol) as fuel. Nine blends were tested by varying diesel (100 to 10% by vol.), biodiesel (80 to 10% by vol.), and keeping ethanol as 10% constant. The brake thermal efficiency, smoke, oxides of nitrogen, carbon dioxide, maximum cylinder pressure, angle of maximum pressure, angle of 5% and 90% mass burning were predicted based on load, speed, diesel, and biodiesel percentage. To validate this regression model another 26.506er multi component fuel comprising diesel-palm methyl ester-ethanol was used in same engine. Statistical analysis was carried out between predicted and experimental data for both fuel. The performance, emission, and combustion characteristics of multi cylinder diesel engine using similar fuel blends can be predicted without any expenses for experimentation.

Key words: diesel, hybrid fuel, European stationary cycle, regression, performance, emission combustion

Introduction

The problems faced by both developing and developed countries which were not having the sources of fossil fuels, leads to an increasing their attention to alternative fuels. The net export income of these countries vanishes to overcome the fossil fuel import. The unpredictable climate change and annual rise of earth temperature attract more attention towards alternative technology. Many research works were carried out with number of techniques for the past two decades to replace diesel fuel either by sole or partially substitutions. Based on the results of these researches, the fuels from bio origin are best suited for existing diesel engine without much modification. These bio origin fuels have three dimensional advantages. The reduction on demand for fossil fuel is first one, even small percentage of replacement can save import considerably. Secondly, the bio fuels are almost oxygenated and hence lesser environmental pollution. Finally, the awareness, attention and cultivation of bio products may increase rural employment, which are regarded as waste land.

The high cetane number, comparable energy content, better lubricity, and higher flash point of biodiesel show its suitability in diesel engine. The slightly higher thermal efficiency and

* Corresponding author; e-mail: rajendirang@sify.com

reduction in emission characteristics like smoke, unburned hydrocarbon, and carbon monoxide were also reported as benefits of biodiesel in diesel engine. However the higher density, lower volatility, higher fuel consumption and increase of oxides of nitrogen emissions were the limiting points of biodiesel. In the case of ethanol which is considered as low cost additive and having 34% oxygen in weight [1]. The lower cetane number, flash point, and poor solubility of ethanol are barrier for its usage in diesel engine. Combining these two different fuels would also adding benefits of these two and compensating drawbacks of each other. The addition of ethanol would improve cold flow properties of the blend [2]. On the other hand the solubility of ethanol will be greatly improved by adding biodiesel without other additives [3]. The multi component fuel comprising diesel, biodiesel and ethanol was tried in diesel engines [4-8]. The performance and emission analysis of these blends were reported. Extensive combustion analysis of these blends and regression model was not reported. Some researchers were worked with regression model [8] and artificial neural networks for existing diesel engine using diesel [9, 10], and diesel-biodiesel blends [11]. In this present investigation, biodiesel from pungamia methyl ester and ethanol were blended with diesel. The performance, combustion and emission analysis of diesel engine were carried out using hybrid blends as fuel.

The experiments were conducted based on 13 mode European stationary cycle. Nine blends were prepared and used for experiments. The percentage of diesel was varied from 100 to 10% by vol. and biodiesel was from 80 to 10% by vol. and keeping ethanol as 10% constant. Based on experimental data, multiple linear regression equations were formed to predict the performance, emission, and combustion characteristic of multicylinder diesel engine using simulation program.

Linear regression equations

The linear equations were formed based on the experimental data [12], which is given in eq. (1):

$$y(x_1, x_2, \dots, x_k) = \beta_0 + \beta_1 x_1 + \beta_2 x_2 + \dots + \beta_n x_n \quad (1)$$

The regression coefficients ($\beta_0, \beta_1, \beta_2, \dots, \beta_n$) were determined from the observed data. The system of linear equations were formed using the correlations (eqs. 2-5):

$$\sum y = \beta_0 n + \beta_1 \sum x_1 + \beta_2 \sum x_2 + \dots + \beta_k \sum x_n \quad (2)$$

$$\sum x_1 y = \beta_0 \sum x_1 + \beta_1 \sum x_1^2 + \beta_2 \sum x_1 x_2 + \dots + \beta_k \sum x_1 x_n \quad (3)$$

$$\sum x_2 y = \beta_0 \sum x_2 + \beta_1 \sum x_2 x_1 + \beta_2 \sum x_2^2 + \dots + \beta_k \sum x_2 x_n \quad (4)$$

$$\sum x_k y = \beta_0 \sum x_k + \beta_1 \sum x_k x_2 + \beta_2 \sum x_k x_2 + \dots + \beta_k \sum x_n^2 \quad (5)$$

This equations were solved using Gauss's elimination with backward substitution method. The linear system of equations based on solving method given by Burden and Faires [13] is formed as:

$$\begin{aligned} E_1: a_{11}\beta_0 + a_{12}\beta_1 + \dots + a_{1n}\beta_n &= b_1 \\ E_2: a_{21}\beta_0 + a_{22}\beta_1 + \dots + a_{2n}\beta_n &= b_2 \\ E_n: a_{n1}\beta_0 + a_{n2}\beta_1 + \dots + a_{nn}\beta_n &= b_n \end{aligned} \quad (6)$$

To solve these equations the augmented matrix \tilde{A} was formed as:

$$\tilde{A} = [A, B] = \begin{bmatrix} a_{11} & a_{12} & \cdots & a_{1n} & \vdots & a_{1,n+1} \\ a_{21} & a_{22} & \cdots & a_{2n} & \vdots & a_{2,n+1} \\ \vdots & \vdots & \vdots & \vdots & \vdots & \vdots \\ a_{n1} & a_{n2} & \cdots & a_{nn} & \vdots & a_{n,n+1} \end{bmatrix} \quad (7)$$

The entries in the $(n + 1)^{\text{th}}$ column are the values of 'b', provided $a_{11} \neq 0$, the corresponding operations $[E_j - (a_{j1}/a_{11})E_1] \rightarrow (E_j)$ were carried for each $j = 2, 3, \dots, n$ to eliminate the coefficient of β_1 in each of these rows. The resulting matrix is in the form:

$$\tilde{A} = \begin{bmatrix} a_{11} & a_{12} & \cdots & a_{1n} & \vdots & a_{1,n+1} \\ 0 & a_{22} & \cdots & a_{2n} & \vdots & a_{2,n+1} \\ \vdots & \ddots & \ddots & \vdots & \vdots & \vdots \\ 0 & \cdots & 0 & a_{nn} & \vdots & a_{n,n+1} \end{bmatrix} \quad (8)$$

The new linear system is triangular in the form of eq. 9.:

$$\begin{aligned} a_{11}\beta_0 + a_{12}\beta_1 + \cdots + a_{1n}\beta_n &= a_{1,n+1} \\ a_{12}\beta_1 + \cdots + a_{2n}\beta_n &= a_{2,n+1} \\ \vdots & \vdots \\ \vdots & \vdots \\ a_{nn}\beta_n &= a_{n,n+1} \end{aligned} \quad (9)$$

Backward substitution can be performed, solving the n^{th} equation for β_n gives eq. 10:

$$\beta_n = \frac{a_{n,n+1}}{a_{nn}} \quad (10)$$

Solving $(n - 1)^{\text{th}}$ equation for β_{n-1} and using the known values of β_n yields:

$$\beta_{n-1} = \frac{a_{n-1,n+1} - a_{n-1,n}\beta_n}{a_{n-1,n-1}} \quad (11)$$

Continuing this process, the β_i in the form of:

$$\beta_i = \frac{a_{i,n+1} - a_{i,nn} - a_{i,n-1}\beta_{n-1} - \cdots - a_{i,i+1}\beta_{i+1}}{a_{ii}} = \frac{a_{i,n+1} - \sum_{j=i+1}^n a_{ij}\beta_j}{a_{ii}} \quad (12)$$

Substituting the value of β_i in eq. (1), the regression equation was formed. These equations can be used to predict the value of dependent variable in terms of independent variables. Statistical analysis to for the regression model and validation of experimental data was also carried out. The regression coefficient (r^2), adjusted correlation coefficient (adj. r^2), standard error of estimate (SEE) and test for significance parameters (t and F value) were also discussed.

Experimental set-up and method

The experiments were conducted in a multi cylinder (six cylinder) water cooled naturally aspirated diesel engine (HINO. An eddy current dynamometer (130 kW capacity) was coupled to the engine with suitable propeller shaft for balancing. The volumetric fuel metering system for fuel flow rate measurement. The air box fitted with orifice and monometer was used for measuring steady flow of inlet air and exhaust gas. The exhaust gas analyzer (AVL Digas 4000) was used to measure the exhaust emissions. The smoke opacity (HSU) was measured with the

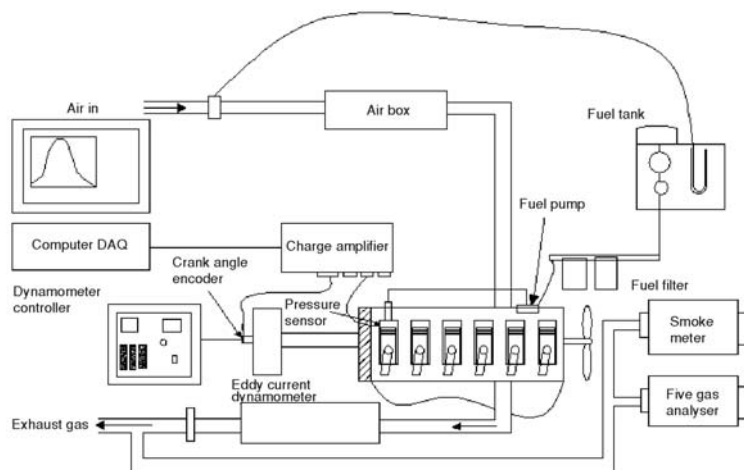


Figure 1. Layout of the experimental set-up

Table 1. Specifications of the engine

Type	4 stroke DI diesel
Make	Ashok Leyland-HINO
Bore	104 mm
Stroke	118 mm
Displacement	6.014 liters
Maximum output	71 kW at 2200rpm
Maximum torque	290 Nm at 1600rpm
Injection timing	20° bTDC
Injection pressure	230 bar

help of continuous flow smoke meter (AVL 437). A piezoelectric pressure transducer was flush mounted in sixth cylinder and the crank angle encoder (AVL 365C) was fitted at the end of the output shaft. The pressure and crank angle signals were conditioned and amplified using four channel charge amplifier. The data acquisition card connected to the personal computer receives the signal from amplifier and converts these signals in to useful data with the help of software. The layout of experimental set-up is shown in fig. 1 and the specifications of the engine are given in tab. 1. The measuring devices and accuracies were given in tab.2.

Table 2. Specifications of the measuring devices

Measuring device	Range	Accuracy
Dynamometer	0-750 Nm	±0.2%
Fuel flow meter	0-500 ml	0.5%
Manometer for inlet air	0-1000 mm of Hg	±2%
Cylinder pressure sensor	0-250 bar	0.1 bar
Crank angle encoder	0-20,000 rpm	0.1° CA
Smoke meter	0-100% opacity	±2%
NO _x	0-5000 ppm	1 ppm
HC	0-20,000 ppm	1 ppm
CO ₂	0-20 vol.%	0.1 vol.%
Calculated parameters		Uncertainties
Brake power		±0.01%
BTE		±0.5%

The experiments conducted based on European stationary cycle (ESC) [14], which is given in fig 2. In fig 2, thirteen modes are given, which is indicated inside the circle. Three speeds (n_a , n_b , and n_c) and four loads (25-100%) are numbered from 2-13. The number 1 is meant for idling speed and no load conditions. The percentage values indicated outside the circle are weighting factors, which are to be multiplied with emissions, eqs. (19)-(21). The three speeds were determined from the correlations [15] given in eqs. (13)-(15).

$$n_a = n_1 + 0.25(n_h - n_1) \quad (13)$$

$$n_b = n_1 + 0.50(n_h - n_1) \quad (14)$$

$$n_c = n_1 + 0.75(n_h - n_1) \quad (15)$$

The high speed (n_h) and low speed (n_l) were determined by calculating 70% and 50% of maximum rated power. Based on the trail experiments conducted in HINO engine, the values of n_a , n_b , and n_c were 1500, 1600, and 1700 rpm. The maximum load specified by the manufacturer is 324 Nm, however the engine was reconditioned and the maximum load obtained was 290 Nm. Hence the four loads 72.5, 145, 217.5, and 290 Nm was chosen for the present work. The units of NO_x , HC, and CO_2 emission were converted from ppm into g/kWh using SAE J177 [16]. The unit conversion from ppm into mass basis g/h for the emissions is given in eqs. (16)-(18):

$$\text{NO}_{x\text{mass}} [\text{gh}^{-1}] = 0.0620 \times \text{NO}_{x\text{conc}} [\text{ppm}] \times m_e \quad (16)$$

$$\text{HC}_{\text{mass}} [\text{gh}^{-1}] = 0.0287 \times \text{HC}_{\text{conc}} [\text{ppm}] \times m_e \quad (17)$$

$$\text{CO}_{2\text{mass}} [\text{gh}^{-1}] = 0.0909 \times \text{CO}_{2\text{conc}} [\text{ppm}] \times m_e \quad (18)$$

The brake specific emissions for entire cycle [$\text{gkW}^{-1}\text{h}^{-1}$] was calculated as follows, eqs. (19)-(21):

$$\text{NO}_x [\text{gkW}^{-1}\text{h}^{-1}] = \frac{\sum(\text{NO}_{x\text{mass}} \times W_f)}{\sum(\text{BP} \times W_f)} \quad (19)$$

$$\text{HC} [\text{gkW}^{-1}\text{h}^{-1}] = \frac{\sum(\text{HC}_{\text{mass}} \times W_f)}{\sum(\text{BP} \times W_f)} \quad (20)$$

$$\text{CO}_2 [\text{gkW}^{-1}\text{h}^{-1}] = \frac{\sum(\text{CO}_{2\text{mass}} \times W_f)}{\sum(\text{BP} \times W_f)} \quad (21)$$

To verify this model, the experimental data of diesel and D60PME30E10 (diesel 60%, PME 30%, and ethanol 10% by vol.) blend was compared with predicted values. The experiments in multi cylinder (HINO) engine using three fuel blends were not carried out formerly. Hence to validate this model a hybrid fuel (D60PAME30E10) comprising diesel-palm methyl ester (PAME)-ethanol was used in the same engine and same operating conditions. For convenience purpose, the thermal efficiency, smoke emission and combustion characteristics of diesel and hybrid fuel blends are discussed for 1600 rpm and 25, 50, 75, and 100% loads. The NO_x , HC and CO_2 emissions for the ESC cycle is discussed as g/kWh.

Result and discussion

Brake thermal efficiency

The linear regression equation to predict the brake thermal efficiency (BTE) in terms of speed (Ne), load (W), diesel (D) and biodiesel (PME) is given in eq. (22):

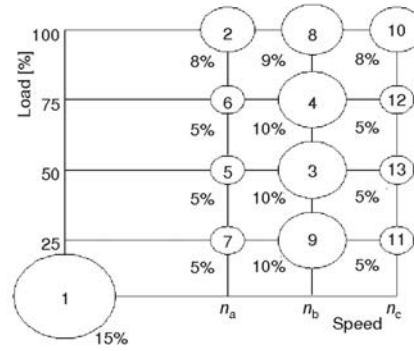


Figure 2. ESC test cycle

$$BTE[\%] = -40.817 + (0.0124N_e) + (0.0689W) + (0.442D) + (0.468PME) \quad (22)$$

The thermal efficiency of an engine depends on the speed, load, heating values, and specific gravity of the fuel. Since the power developed is directly proportional to speed and load. It is expected great influence on BTE. The specific gravity of the fuel is inversely proportional on BTE, higher specific gravity leads to lower BTE. The regression coefficient (r^2), adjusted regression coefficient, and standard error of estimate (SEE) for predicting equations were given in tab. 3. In the eq. (22) the load and speed have larger influence on predicting brake thermal efficiency of the engine, their test of significant (t) values were 22.677 and 13.170, respectively. The thermal efficiency of the engine operated with diesel is slightly higher than blended fuels (fig. 3). This may be due to lower heating value of the biodiesel (12% and 8% lower than diesel for PME and PAME) and ethanol (40% lower than diesel) in the blend. The standard error of estimate for brake thermal efficiency of an engine operated with diesel, PME and PAME blends were 1.996, 1.824, and 1.721, respectively. The r^2 value of diesel, PME, and PAME blends were 0.958, 0.952, and 0.96, respectively. This analysis shows that all the three fuels are good agreement with the regression eq. (22).

Table 3. Statistical results of predicting equations

Parameter	r^2	Adj. r^2	SEE
BTE	0.960	0.918	2.45
Smoke	0.921	0.843	5.455
NO _x	0.945	0.973	32.870
HC	0.706	0.692	0.364
CO ₂	0.949	0.947	2123.078
P _{max}	0.973	0.946	1.580
AP _{max}	0.959	0.916	0.383
AI05	0.828	0.822	0.388
AI90	0.963	0.962	1.159

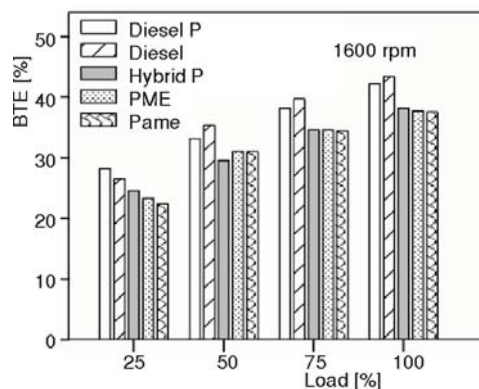


Figure 3. Brake thermal efficiency

Smoke emissions

The predicting equation for smoke emission is given in eq. 23.

$$\text{Smoke}(HSU) = 8.874 - 0.00260N_e + 0.142W - 0.0469D + 0.0140PME \quad (23)$$

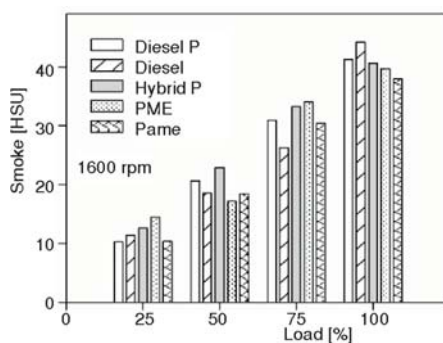


Figure 4. Smoke emission

In this equation load alone has a larger influence on predicting smoke value of an engine, its ' t ' value was 22.236. It can be seen from fig. 4, the smoke emissions are increases drastically with load. This may be due to the relatively lower air-fuel ratio at higher loads when larger quantity of fuel is injected [17]. The speed of the engine and fuel content were lesser effects on smoke formation, their significant values were -1.310 for speed, 0.245 for diesel, and 0.0682 for biodiesel. The comparison of smoke emissions of the engine operated with diesel, and hybrid fuel blends is shown in fig. 4. The standard error

of estimate for smoke of an engine operated with diesel, PME, and PAME blends were 4.35, 3.14, and 2.96, respectively. Due to the presence of oxygen concentration of blended fuels the lower smoke emission was observed. The correlation coefficient of diesel, PME, and PAME blends were 0.904, 0.937, and 0.942, respectively.

Oxides of nitrogen (NO_x)

The oxide of nitrogen emission of an engine is determined by peak combustion temperature, pressure and oxygen concentration [17]. The NO_x emission for each mode in terms of speed (N_e), load (W), diesel (D) and biodiesel (PME) is given in eq. (24):

$$NO_x [gh^{-1}] = -285.482 + 0.0654N_e + 1.356W + 2.793D + 2.679PME \quad (24)$$

The load ($t = 35.002$) on the engine was more influencing on predicting NO_x emissions than other variables. The comparison of NO_x emissions for diesel and hybrid fuel blends for ESC cycle is shown in fig. 5. The NO_x emissions for PME and PAME based hybrid fuel were 1.8 and 10.18% lower than diesel fuel for the cycle. This may be due to lower heating value of biodiesel and ethanol in the blend is expected to lowdown the pressure and temperature. The standard error of estimate for NO_x of an engine operated with diesel, PME and PAME blends were 40.01, 35.12, and 18.71, respectively. It is also noticed from the figure, the NO_x of the engine is more influenced by its load. The correlation coefficient of diesel, PME, and PAME blends were 0.901, 0.935, and 0.973, respectively.

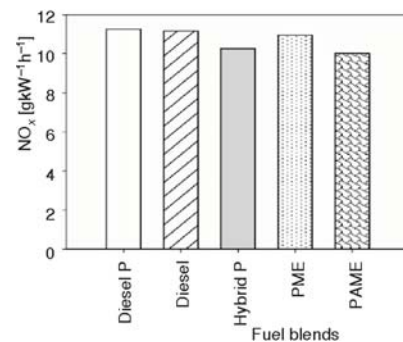


Figure 5. NO_x emission for ESC cycle

Hydrocarbon (HC)

The hydrocarbon emission from the engine is determined latent heat of vaporization, combustion pressure and temperature. The HC emission for each mode in terms of speed (N_e), load (W), diesel (D) and biodiesel (PME) is given in eq. (25):

$$HC [gh^{-1}] = 7342 + 0.00115N_e + 0.00116W - 0.0695D - 0.0763PME \quad (25)$$

The speed ($t = 8.696$) of the engine was more influencing on predicting HC emissions than other variables. The HC emissions for PME and PAME based hybrid fuel were 21.65 and 15.31% higher than diesel fuel for the cycle (fig. 6). This may be due to the presence of ethanol in the blend which has high latent heat of vaporization than diesel [18] and biodiesel and hence higher HC emissions were observed. The standard error of estimate for HC emission of an engine operated with diesel, PME and PAME blends were 0.106, 0.172, and 0.146, respectively. The correlation coefficient of diesel, PME and PAME blends were 0.78, 0.77, and 0.76, respectively. The deviation between predicted and experimental values for diesel and PME blend was negligible and PAME blend was 5.3%.

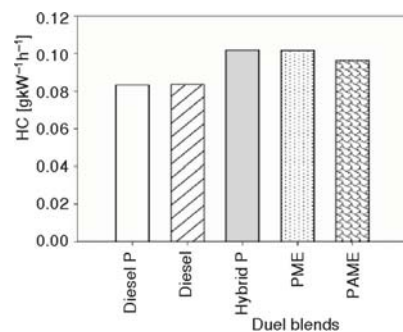


Figure 6. HC emission for ESC cycle

Carbon dioxide emission (CO_2)

The CO_2 emission of an engine depends on oxygen content and temperature of the combustion chamber. The linear regression equation for predicting CO_2 emission is given in eq. (26):

$$CO_2 [gh^{-1}] = -1348963 + 6.427N_e + 87975W - 17917D - 123848PME \quad (26)$$

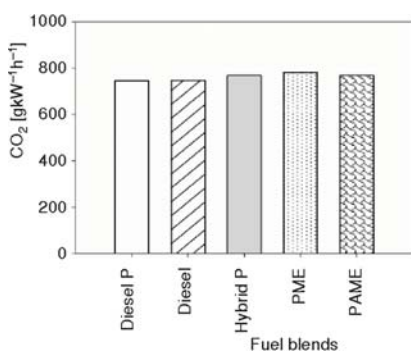


Figure 7. CO_2 emission for ESC cycle

This statistical analysis also shows the 't' value for load was 35.155 and 8.326 for speed, -0.240 for diesel and -0.173 for biodiesel. The CO_2 emissions for the hybrid fuel blends are higher than diesel (fig. 7). The more oxygen content of the biodiesel improves the combustion of blended fuel [19]. An average of 4.88 and 2.99% higher CO_2 emissions were observed with PME and PAME blends than diesel. The standard error of estimate for CO_2 emissions were 2712.4, 2348.08, and 1397.83 for diesel, PME, and PAME blends. The r^2 value of diesel, PME, and PAME blends were 0.877, 0.926, and 0.963, respectively. It may be noted from the figure the difference between predicted and experimental CO_2 emissions were negligible for all the fuels.

Maximum cylinder pressure (P_{max})

The peak cylinder pressure depends on the load, speed and the amount of fuel burned during premixed combustion stage. Equation (27) gives the prediction of maximum cylinder pressure.

$$P_{max} [\text{bar}] = 38.147 + 0.0113N_e + 0.0473W + 0.0253D + 0.0191PME \quad (27)$$

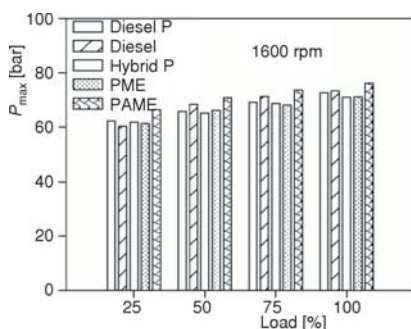


Figure 8. Maximum cylinder pressure

The peak cylinder pressure increase with load and speed, this is due to higher residual gas temperature and wall temperature at higher loads [20]. In this equation the load and speed have larger influence on predicting P_{max} of an engine, their 't' values were 25.541 and 19.752, respectively. The P_{max} for diesel and blended fuels are compared in fig. 8. The standard error of estimate for P_{max} of an engine operated with diesel, PME and PAME blends were 1.751, 1.225, and 1.596, respectively. It is also noticed from the figure, the maximum cylinder pressure of the engine is more influenced by load and speed of the engine. The peak cylinder for PAME blended fuel is higher than diesel and PME blended fuel. The correlation coefficient of diesel, PME and PAME blends were 0.92, 0.957, and 0.931, respectively.

Crank angle of maximum pressure (AP_{max})

The angle of maximum cylinder pressure is mainly influenced by rate of combustion and ignition delay [21]. Equation (28) gives the prediction of AP_{max} influenced by other variables:

$$AP_{\max} [\text{deg.}] = 5.090 + 0.00304N_e + 0.00604W - 0.0605D - 0.0622PME \quad (28)$$

In this equation the load and speed have larger influence on predicting AP_{\max} , their 't' values were 13.475 and 21.863, respectively. The predicted and experimental AP_{\max} of the engine for diesel and blended fuel is shown in fig. 9. The peak pressure appears earlier for diesel fuel than fuel blends. This may be due to lower rate of combustion for hybrid fuel blends than diesel. The standard error of estimate for AP_{\max} of an engine operated with diesel, PME, and PAME blends were 0.235, 0.192, and 0.178, respectively. The r^2 value for diesel, PME, and PAME blends were 0.902, 0.973, and 0.969.

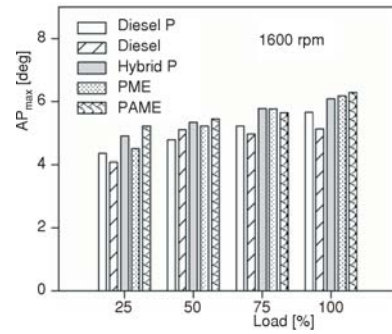


Figure 9. Angle of maximum pressure

Angle of 5% mass burning (AI05)

The angle of 5% mass burning ($AI05$) is taken as SOC for this present investigation. The linear regression equation for 5% mass burning is given in eq. (29):

$$AI05 [\text{deg.}] = 2.182 + 0.00142N_e + 0.00492W - 0.0941D - 0.112PME \quad (29)$$

In this equation the load and speed have larger influence on predicting $AI05$ of an engine, their 't' values were 10.814 and 10.083, respectively. The ignition delay is decreased with increasing load for all the fuels. When the load increases the gas temperature inside the combustion chamber will increase because of higher engine load, which will reduce the physical delay of any fuel [21]. The fuel content has least effect on predicting $AI05$ when compared to speed and load. The angle of 5% mass burning is lower for biodiesel blended fuels than diesel (fig.10). This may be due to complex and rapid pre-flame chemical reactions takes place for hybrid fuel blends. The standard error of estimate for $AI05$ of an engine operated with diesel fuel was 0.209, PME in the blend was 0.221 and PAME in the blend was 0.115. The correlation coefficient of diesel, PME, and PAME blends were 0.832, 0.852, and 0.944, respectively. This shows that the equation is highly suitable for PAME blend than other blends.

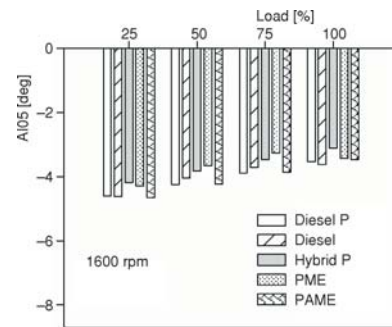


Figure 10. Angle of 5 % mass burning

Angle of 90% mass burning (AI90)

The crank angle of 90% heat release ($AI90$), indicates the end of combustion in the same way that $AI05$ indicates the start of combustion. The last 10% mass burning is not considered due to error associated with the assumption made in the heat release analysis [22]. The prediction equation for $AI90$ of different fuel blends is given in eq. 30:

$$AI90[\text{deg}] = 35.907 + 0.0129N_e + 0.0307W - 0.440D - 0.451PME \quad (30)$$

In this equation the speed and load have larger influence on predicting $AI90$ of an engine, their 't' values were 30.572, and 22.623, respectively. The fuel content has least effect on predicting $AI90$ (t value of diesel was -10.802 and PME was -10.334) when compared to speed

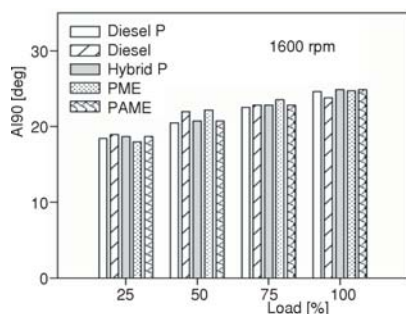


Figure 11. Angle of 90% mass burning

and load. The AI_{90} increases with load, because of larger quantities of fuel need to be injected for higher loads. The angle of 90% mass burning of the engine operated with diesel and blended fuel is compared in fig. 11. The standard error of estimate for AI_{90} of an engine operated with diesel, PME and PAME blends were 0.804, 1.02, and 0.641, respectively. As discussed earlier the combustion ends earlier for hybrid fuel blends. However for calculating combustion duration ($AI_{90}-AI_{05}$) the pungamia bio-diesel blended fuel is higher than diesel fuel. At 1600 rpm and full load condition, the combustion duration for diesel fuel is 27.41° CA, whereas for PME and PAME blended fuels are 28.11 and 28.31° CA. The r^2 values for diesel, PME, and PAME blends were 0.93, 0.890, and 0.944, respectively.

Conclusions

The experiments were conducted in a multi cylinder direct injected diesel engine using diesel and diesel-pungamia methyl ester-ethanol as fuel. Based on the experimental data, multiple linear regression equations were formed to predict the performance, emission and combustion characteristics of these blended fuels. Statistical analysis of these equations gives r^2 and adj. r^2 almost nearer to 1. The standard error of estimate for brake thermal efficiency, smoke, NO_x , HC, CO_2 , P_{max} , AP_{max} , AI_{05} , and AI_{90} are 2.45, 0.921, 32.870, 0.364, 2123.07, 1.580, 0.383, 0.388, and 1.159, respectively. To validate this model, another hybrid fuel comprising diesel-palm methyl ester-ethanol was used as fuel in the same engine. The experimental and predicted value of this blend was also correlated with the regression equations. These equations can be used in multi cylinder diesel engine (HINO) to get information on performance, emission, and combustion characteristics using hybrid fuel blends without any expenses for experimentation.

Acknowledgment

Authors thank Department of Science and Technology, Govt. of India for sponsoring the research project "Indigenous resource utilization: development of diesel-ethanol – vegetable oil hybrid fuel blends and field testing in commercial transport vehicles".

References

- [1] Hulwan, D. B., Joshi, S. V., Performance, Emission and Combustion Characteristics of a Multicylinder DI Diesel Engine Running on Diesel-Ethanol-Biodiesel Blends of High Ethanol Content, *Applied Energy*, 88 (2011), 12, pp. 5042-5055
- [2] Shi, X., et al., Emission Characteristics Using Methyl Soyate-Ethanol-Diesel Fuel Blends on a Diesel Engine, *Fuel*, 84 (2005), 12-13, pp. 1543-1549
- [3] McCormick, R. L., Parish, R., Technical Barriers to the Use of Ethanol in Diesel Fuel, Milestone Report to NREL/MP-540-32674, 2001
- [4] Celikten, I., The Effect of Biodiesel, Ethanol and Diesel Fuel Blends on the Performance and Exhaust Emissions in a DI Diesel Engine, *Gazi University Journal of Science*, 24 (2011), 2, pp. 341-346
- [5] Labeckas, G., et al., Performance and Exhaust Emission Characteristics of Diesel Engine Fuelled with Ethanol-Diesel-Biodiesel Blend, *Proceedings, International Scientific Conference Engineering for Rural Development*, Jelgava, Latvia, 2005, pp. 266-271

- [6] Singh, P. J., *et al.*, Preparation, Characterisation, Engine Performance and Emission Characteristics of Coconut Oil Based Hybrid Fuels, *Renewable Energy*, 35 (2010), 9, pp. 2065-2070
- [7] Altun, S., *et al.*, Effect of a Mixture of Biodiesel-Diesel-Ethanol as Fuel on Diesel Engine Emissions, *Proceedings*, 6th International Advanced Technologies Symposium, Elazig, Turkey, pp. 5-7
- [8] Ali, Y., *et al.*, Optimization of Diesel, Methyl Tallowate and Ethanol Blend for Reducing Emissions from Diesel Engine, *Bioresource Technology*, 52 (1995), 3, pp. 237-243
- [9] Ozener, O., *et al.*, Artificial Neural Network Approach to Predicting Engine-Out Emissions and Performance Parameters of a Turbo Charged Diesel Engine, *Thermal Science*, 17 (2013), 1, pp. 153-166
- [10] Naradasu, R. K., *et al.*, Towards Artificial Intelligence Based Diesel Engine Performance Control under Varying Operating Conditions Using Support Vector Regression, *Thermal Science*, 17 (2013), 1, pp. 167-178
- [11] Ganapathy, T., *et al.*, Artificial Neural Network Modeling of Jatropha Oil Fueled Diesel Engine for Emission Predictions, *Thermal Science*, 13 (2009), 3, pp. 91-102
- [12] Walpole, R. E., *et al.*, *Probability & Statistics for Engineers and Scientists*, Pearson education, London, 2002
- [13] Burden, R. L., Faires, J. D., *Numerical Analysis Theory and Applications*, Cengage Learning India Pvt. Ltd., New Delh, 2010
- [14] Kim, H., Choi, B., The Effect of Biodiesel and Bioethanol Blended Diesel Fuel on Nanoparticles and Exhaust Emissions from CRDI Diesel Engine, *Renewable Energy*, 35 (2010), 1, pp. 157-163
- [15] Kegl, B., Effects of Biodiesel on Emissions of a Bus Diesel Engine, *Bioresource Technology*, 99 (2008), 4, pp. 863-873
- [16] ***, *Engine Fuel and Lubrication, J177-Measurement of Carbon Dioxide, Carbon Monoxide, and Oxides of Nitrogen in Diesel Exhaust*, SAE Handbook, 3, 1985
- [17] Agarwal, A.K, Rajamanoharan, K., Experimental Investigations of Performance and Emissions of Karanja Oil and its Blends in a Single Cylinder Agricultural Diesel Engine, *Applied Energy*, 86 (2009), 1, pp. 106-112
- [18] Jagadish, D., *et al.*, The Effect of Supercharging on Performance and Emission Characteristics of Compression Ignition Engine with Diesel-Ethanol-Ester Blends, *Thermal Science*, 15 (2011), 4, pp. 1165-1174
- [19] Chauhan, *et al.*, A Study on the Performance and Emission of a Diesel Engine Fueled with Karanja Biodiesel and its Blends, *Energy*, 56 (2013), 1, pp. 1-7
- [20] Rajendiran, G., *et al.*, Experimental Investigation on Combustion Analysis of Multicylinder Direct Injected Diesel Engine Using Diesel-Biodiesel-DEE as Alternative Fuel, *International Journal of Ambient Energy*, 34 (2013), 2, pp. 63-72
- [21] Sinha, S., Agarwal, A. K., Experimental Investigation of the Combustion Characteristics of a Biodiesel (Rice-Bran Oil Methyl Ester)-Fuelled Direct-Injection Transportation Diesel Engine, *Journal of Automobile Engg.*, 221 (2007), 8, pp. 921-932
- [22] Ali, Y., *et al.*, Effect of Alternative Diesel Fuels on Heat Release Curves for Cummins N14-410 Diesel Engine, *Transactions of ASAE*, 39 (1996), 2, pp. 407-414